The unusual temperature dependence of the switching behavior in a ferroelectric single crystal with dislocations

The unusual temperature dependence of the switching behavior in a ferroelectric single crystal with dislocations

H H Wu[1], J Wang[2], S G Cao[1], L Q Chen[3] and T Y Zhang[1]

[1] Department of Mechanical and Aerospace Engineering, The Hong Kong University of Science and Technology, Clear Water Bay, Kowloon, Hong Kong, People's Republic of China
[2] Department of Engineering Mechanics, School of Aeronautics and Astronautics, Zhejiang University, Hangzhou 310027, People's Republic of China
[3] Department of Materials Science and Engineering, The Pennsylvania State University, University Park, PA 16802, USA

E-mail: mezhangt@ust.hk

Abstract

The unusual temperature-induced switching behavior in a ferroelectric single crystal with dislocation arrays is investigated by using phase field simulations. The results show that the influence of temperature on the hysteresis loop of a ferroelectric is dependent on the dislocation arrays. In the presence of dislocation arrays, the dependence of the coercive field on the temperature is different from that of a dislocation-free ferroelectric. The coercive field increases when the temperature increases from room temperature to a critical temperature, which is attributed to the pinning of domains by the dislocation arrays. Above the critical temperature, both the coercive field and the remnant polarization decrease with temperature. It is found that double hysteresis loops can be induced by dislocation arrays when the temperature is higher than the Curie temperature. This work exhibits the complex role of temperature and dislocations in the polarization switching of ferroelectric single crystal.

S Online supplementary data available from stacks.iop.org/SMS/23/025004/mmedia

(Some figures may appear in colour only in the online journal)

1. Introduction

Ferroelectrics are widely used in capacitors, sensors, and actuators [1, 2] due to their excellent dielectric and electromechanical response to an external electric field. The macroscopic electromechanical properties of ferroelectric materials, such as the remnant polarization and the coercive field, are related to the switching dynamics of polarization and are highly dependent on the environmental temperature. According to the thermodynamic theory of ferroelectric materials, the spontaneous polarization becomes smaller when the temperature increases. Correspondingly, the macroscopic remnant polarization and coercive field decrease with increase in temperature. However, in the presence of defects, such as point charges and dislocations, the effect of temperature on the remnant polarization and coercive field becomes complex. Therefore, a full understanding of the temperature dependence of ferroelectric properties is important not only for technological applications but also for fundamental understanding.

Due to the complex nature of real experiments, the effects of temperature on the properties of ferroelectric material are inconsistent in different experiments. Based on the conventional mixed-oxide technique, Khemakhema *et al* [3] measured the polarization hysteresis loops of the $BaTi_{0.975}(Zn_{1/3}Nb_{2/3})_{0.025}O_3$ ceramic at different

temperatures and found that the remnant polarization and coercive field decrease when the temperature increases from 280 to 330 K. Similar results have been found by many researchers [4–10], and are reasonable from the thermodynamics point of view.

However, unusual temperature effects on the remnant polarization and coercive field have been observed in some experiments. For example, both the dielectric constant and the remnant polarization of $Sr_{0.97}Bi_{1.61}Ta_2O_9$ and $Sr_{0.83}Bi_{2.08}Ta_2O_9$ thin films increased with increasing temperature in the temperature range from 100 to 300 K [11], which was attributed to the difficulty of polarization switching at lower temperatures with low applied electric field. The increase of macroscopic remnant polarization with temperature contradicts thermodynamic theory.

Recently, high temperature piezoresponse force microscopy (PFM) [12] was used to measure the piezoresponse hysteresis loops of $PbZr_{0.2}Ti_{0.8}O_3$ films over the temperature range of 25–400 °C. When temperature increases, the piezoresponse increases first and then rapidly decreases near 400 °C, which also conflicts with the thermodynamic theory. The underlying mechanism that leads to the improved piezoresponse by increasing temperature is not clear. Similar unusual phenomena have also been reported in recent decades [13–16]. Although some papers have tried to explain the unusual phenomena by the kinetic effect [11], electrical defects [13–15], and leakage current [16], a direct observation has not been reported yet. In this work, the effect of mechanical defects (dislocations) on the unusual temperature-dependent behavior is explored by phase field simulation.

2. Simulation methodology

The paraelectric to ferroelectric phase transition occurs in a ferroelectric material when the temperature is lower than the Curie point. The polarization, $\mathbf{P} = (P_1, P_2, P_3)$, is usually used as the order parameter to describe the ferroelectric phase transition. In the phase field model of ferroelectrics, the total energy is expressed as a function of the polarization, polarization gradients, strain and electric field. The domain configuration and polarization switching are direct consequences of the minimization process of the total free energy of the whole simulated system. The temporal evolution of the polarization can be described by the time-dependent Ginzburg–Landau (TDGL) equations,

$$\frac{\partial P_i(\boldsymbol{x}, t)}{\partial t} = -L \frac{\delta F}{\delta P_i(\boldsymbol{x}, t)} \qquad (i = 1, 2, 3), \qquad (1)$$

where L is the kinetic coefficient and F is the total energy of the system. $\delta F / \delta P_i(\boldsymbol{x}, t)$ is the thermodynamic driving force for the spatial and temporal evolution of $P_i(\boldsymbol{x}, t)$, and $\boldsymbol{x}$ denotes the spatial vector, $\boldsymbol{x} = (x_1, x_2, x_3)$. The total free energy of equation (1) can be expressed as

$$F = \int_V [f_{\text{Land}}(P_i) + f_{\text{elas}}(P_i, \varepsilon_{ij})$$
$$+ f_{\text{grad}}(P_{i,j}) + f_{\text{elec}}(P_i, E_i, E_i^{\text{ex}})]dV, \qquad (2)$$

in which f_{Land} is the Landau free energy density, which is given by

$$f_{\text{Land}}(P_i) = \alpha_1 \sum_i P_i^2 + \alpha_{11} \sum_i P_i^4 + \alpha_{12} \sum_{i>j} P_i^2 P_j^2$$
$$+ \alpha_{111} \sum_i P_i^6 + \alpha_{112} \sum_{i>j} (P_i^4 P_j^2 + P_i^2 P_j^4)$$
$$+ \alpha_{123} \prod_i P_i^2, \qquad (3)$$

where $\alpha_{11}, \alpha_{12}, \alpha_{111}, \alpha_{112}, \alpha_{123}$ are Landau coefficients and $\alpha_1 = (T - T_0)/2\varepsilon_0 C_0$, T and T_0 denote the temperature and Curie–Weiss temperature, respectively, C_0 is the Curie constant, and ε_0 is the dielectric constant of vacuum. The elastic energy density has the form $f_{\text{elas}} = \frac{1}{2} c_{ijkl}(\varepsilon_{ij} - \varepsilon_{ij}^0 + \varepsilon_{ij}^d)(\varepsilon_{kl} - \varepsilon_{kl}^0 + \varepsilon_{kl}^d)$, where c_{ijkl} are the elastic constants, ε_{ij} are the total strains, and ε_{ij}^0 are the spontaneous strains, which are related to the polarization components in the form of $\varepsilon_{ij}^0 = Q_{ijkl}P_k P_l$ with Q_{ijkl} being the electrostrictive coefficients. Note that the elastic strain induced by the polarization is obtained analytically in Fourier space with the periodic boundary condition [20, 21]. The strain fields of dislocations ε_{ij}^d are obtained from the Stroh formalism and added to the total elastic strain by superposition [22–24]. In addition to the inhomogeneous strain field, charge inhomogeneity induced by dislocations may also influence the switching behavior. In this work, we only consider the mechanical effect of dislocations. The charge effect of dislocations will be investigated in our future work. The gradient energy density gauges the energy penalty for spatially inhomogeneous polarization and is expressed as $f_{\text{grad}} = \frac{1}{2} g_{ijkl}(\partial P_i / \partial x_j)(\partial P_k / \partial x_l)$, where g_{ijkl} is the gradient energy coefficient. The electrical energy density includes the self-electrostatic energy density and the energy induced by the external electric field, which can be expressed as $f_{\text{elec}} = -\frac{1}{2} E_i P_i - E_i^{\text{ex}} P_i$, where E_i and E_i^{ex} are the self-electrostatic electric field and external applied electric field, respectively. The self-electrostatic field is the negative gradient of the electrostatic potential, i.e. $E_i = -\partial \phi / \partial x_i$. The electrostatic potential is obtained by solving the following electrostatic equilibrium equation:

$$\varepsilon_0 \left(\kappa_{11} \frac{\partial^2 \Phi}{\partial x_1^2} + \kappa_{22} \frac{\partial^2 \Phi}{\partial x_2^2} + \kappa_{33} \frac{\partial^2 \Phi}{\partial x_3^2} \right)$$
$$= \frac{\partial P_1}{\partial x_1} + \frac{\partial P_2}{\partial x_2} + \frac{\partial P_3}{\partial x_3}, \qquad (4)$$

where κ_{ij} are the background dielectric constants of the material [25–29]. The semi-implicit Fourier-spectral method is employed to solve the partial differential equation (1) in this work [30].

Although phase field simulations have been employed to investigate the role of dislocations in the domain switching process [17–19], an understanding of the temperature-dependent behavior of ferroelectrics is still lacking. In this study, two-dimensional (2D) simulations are conducted under the plane strain condition. A schematic drawing of the simulated 2D ferroelectric single crystal with dislocation arrays is shown in figure 1, in which the dislocation density
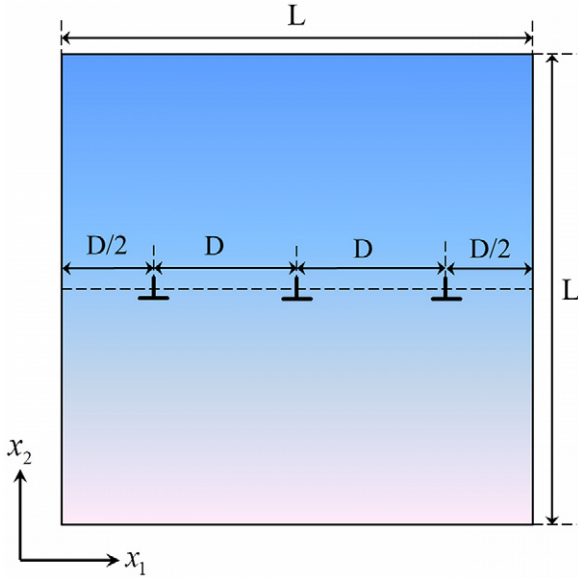
Figure 1. The schematic drawing of the simulated 2D ferroelectric single crystal with dislocation arrays.

is controlled by the distance D between two neighboring dislocations. We define the dislocation linear density (DLD) as L/D. Discrete grids of 64×64 are used for the ferroelectric single crystal with a normalized cell size of $\Delta x_1^* = \Delta x_2^* = 0.8$ and the periodic boundary condition is adopted in both the x_1 and x_2 directions. The normalized formula for all variables, and all material constants of PbTiO$_3$ single crystal used in the simulation can be found in the previous work [20, 21]. The Burgers vectors of dislocations are assumed to be along the x_1 direction. Due to the brittle nature of ceramics, the motion of dislocations in PbTiO$_3$ materials is very difficult at temperatures below the Curie temperature. Dislocations are assumed to remain stationary during the polarization switching. The external sinusoidal electric field $E_2^{\text{ex},*} = E_0^* \sin(4.5\pi i/180\,000)$ is applied along the x_2 direction, where i is an integer denoting the time step. Under each applied electric field at a given time step i, the simulated ferroelectric thin film is allowed to evolve one step with a dimensionless step time of $\Delta t^* = 0.04$. The average polarization along the electric field direction is taken as the macroscopic response of the simulated ferroelectric single crystal.

3. Results and discussion

Figure 2 shows the simulated hysteresis loops of dislocation-free ferroelectric single crystal under different temperatures with an electric field amplitude of $E_0^* = 0.5$, where the polarization is normalized by the magnitude of the spontaneous polarization at room temperature, $P_0 = |\mathbf{P}_0| = 0.757$ C m^{-2}, and the applied field is normalized by $|\alpha_1|P_0$ with $\alpha_1 = \frac{T-T_0}{2\varepsilon_0 C_0} = (25 - 479) \times 3.8 \times 10^5$ m^2 N C^{-2} being the reference Landau coefficient at room temperature, and $E_0^* = E_0/(|\alpha_1|P_0)$ is the dimensionless applied electric field amplitude. The dimensionless polarization and applied electric field are used to express the simulation results
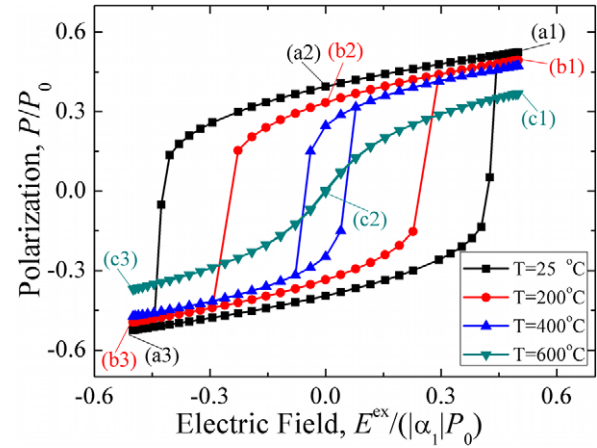

Figure 2. The phase field simulation of the hysteresis loops of a dislocation-free multi-domain ferroelectric under different temperatures. The points marked (a1), (b1) and (c1) on the hysteresis loop correspond to the maximum applied electric field; the points marked (a2), (b2) and (c2) correspond to zero applied electric field; the points marked (a3), (b3) and (c3) correspond to the minimum applied electric field. $P_0 = |\mathbf{P}_0| = 0.757$ C m^{-2} is the magnitude of the spontaneous polarization at room temperature, $\alpha_1 = \frac{T-T_0}{2\varepsilon_0 C_0} = (25 - 479) \times 3.8 \times 10^5$ m^2 N C^{-2} is the reference Landau coefficient at room temperature.

hereafter. From the hysteresis loops, it is found that both the remnant polarization and coercive field decrease as temperature increases. From the hysteresis loops, it is found that both the remnant polarization and the coercive field decrease as the temperature increases. When the temperature is higher than the Curie temperature, the ferroelectric material will behave as a paraelectric. Therefore, the response of polarization to electric field becomes a nonlinear line rather than a hysteresis loop when the temperature increases to 600 °C. The dependence of the remnant polarization and coercive field on the temperature in figure 2 is consistent with the analytic predictions from Landau theory and many experimental observations [3–10].

Figure 3 shows the domain structures at different points of the hysteresis loops in figure 2. It is found that polarizations form typical 90° domain structures when the temperature is lower than the Curie temperature, as shown in figures 3(a1)–(a3) and (b1)–(b3). The domain structures in figures 3(a1)–(a3) correspond to points (a1)–(a3) in figure 2 at positive maximum electric field, zero electric field and negative maximum electric field, respectively. From point (a1) to point (a2), the average polarization in figure 2 decreases a little and the corresponding domain structures from figures 3(a1) to (a2) have a very small variation. The domain pattern does change and only the vertical domains shrink a little. Comparison of figures 3(a3)–(a2) indicates that the domain pattern varies greatly when the electric field changes from zero to the negative maximum value. The polarizations in the middle domain change from the horizontal orientation in figure 3(a2) to the vertical orientation in figure 3(a3). At a temperature of 200 °C, figures 3(b1)–(b3) show a similar evolution of domain structures to that at
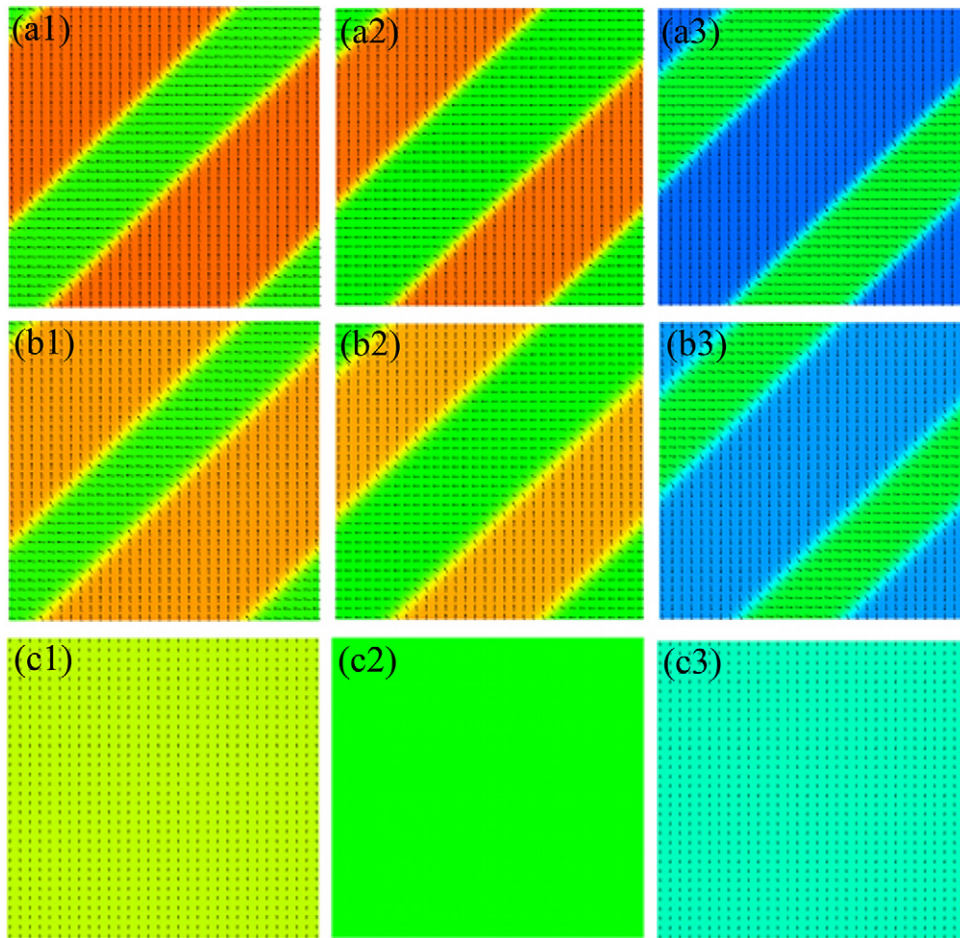
Figure 3. The domain structures of (a1), (a2) and (a3) correspond to the points on the curve of $T = 25\,°C$ in figure 2, respectively; (b1), (b2) and (b3) correspond to the points on the curve of $T = 200\,°C$; (c1), (c2) and (c3) correspond to the points on the curve of $T = 600\,°C$, respectively.

room temperature in figures 3(a1)–(a3). When the temperature increases to 600 °C, however, the polarization is zero at zero electric field, as shown in figure 3(c2). For the positive and negative maximum electric fields, polarizations appear and form a single domain, as shown in figures 3(c1) and (c3).

Figure 4(A) shows the temperature dependence of hysteresis loops of the ferroelectric single crystal with a DLD of 21, where the applied electric field amplitude is 0.7. It is found that both the remnant polarization and the coercive field increase when the temperature increases from room temperature to 200 °C. The unusual temperature dependence of the remnant polarization and coercive field is opposite to those of single domain ferroelectrics and multi-domain ferroelectrics without dislocation arrays in figure 2. With temperature further increasing, both the remnant polarization and the coercive field decrease, which is consistent with the result in figure 2. Interestingly, a double hysteresis loop is obtained at a temperature of $T = 600\,°C$, whereas a nonlinear curve is obtained for ferroelectrics without dislocation arrays, as shown in the figure at $T = 600\,°C$. The observed double hysteresis loop is often attributed to the presence of a nonpolar phase [5, 31] or phase transformation [34]. This work presents a new mechanism in that the local mechanical

inhomogeneity caused by dislocations can also induce the double hysteresis loop. In other words, this work provides an alternative microstructural explanation of the related experimental results. Although the unusual temperature dependence of the remnant polarization and coercive field has been widely reported [11–16], direct observation of the microscopic mechanism has rarely been reported. The present phase field simulations show that the existence of dislocation arrays in ferroelectrics is one of the reasons for the unusual phenomenon. The dependence of the remnant polarization on the temperature is also related to the applied electric field amplitude in the hysteresis loops. Figure 4(B) shows the temperature dependence of the hysteresis loops of ferroelectric single crystal when the applied electric field amplitude reaches 0.8. When the temperature increases from 25 to 200 °C, the coercive field increases while the remnant polarization decreases. The results imply that the temperature dependence of the hysteresis loop in ferroelectrics is not only related to defects but also influenced by the applied electric field amplitude.

Comparing figure 3 with figure 5, there are two significant differences. Firstly, the domain patterns are totally different in the two cases. Secondly, the polarization magnitude is
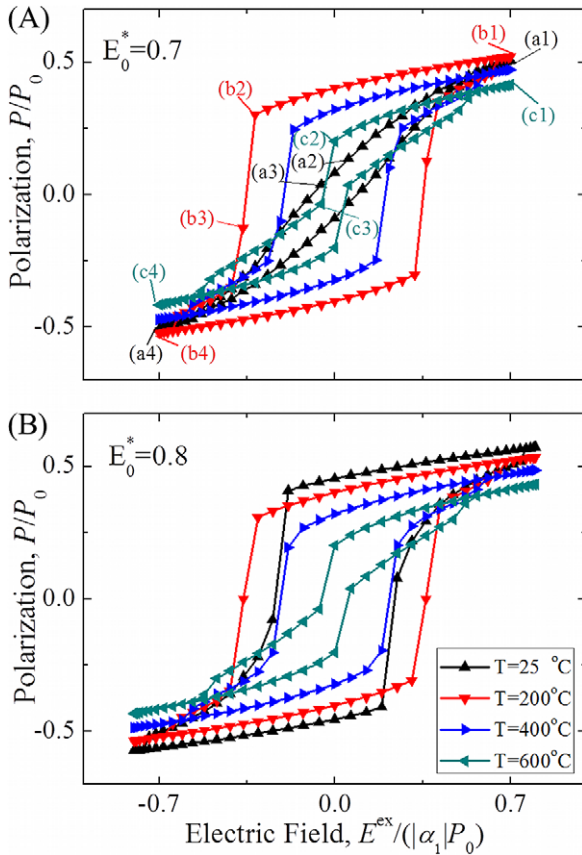
Figure 4. The effect of temperature on the hysteresis loop of a ferroelectric with DLD = 21: (A) at an applied electric field amplitude $E_0^* = 0.7$ and (B) at an applied electric field amplitude $E_0^* = 0.8$. The points marked (a1), (b1) and (c1) on the hysteresis loop correspond to the maximum applied electric field, the points marked (a2)–(a3), (b2)–(b3) and (c2)–(c3) correspond to the two points around the coercive field, the points marked (a4), (b4) and (c4) correspond to the minimum applied electric field. $E_0^* = E_0/(|\alpha_1|P_0)$ is the dimensionless applied electric field amplitude.

almost the same at different locations in figure 3, while it is larger near the dislocation wall than that at other locations in figure 5. The differences are responsible for the unusual temperature dependence of the hysteresis loops. For the case of room temperature, the domain above the dislocation array is firmly pinned by the dislocation array at the maximum electric field, as shown in figures 5(a1) and (a4). Due to the pinning of domains with opposite polarization, growth of the opposite domain takes place when the electric field decreases. Around zero field, the size of opposite domains is close to that of positive domains, as shown in figure 5(a2), which makes the remnant polarization relatively low at $T = 25\,°C$, as shown in figure 4(A). When the temperature increases to $200\,°C$, the domains above the dislocation array are able to form a single domain under the maximum electric field, as shown in figures 5(b1) and (b4), indicating the temperature effect on the depinning of polarizations from the dislocation array. Correspondingly, there is no growth of the opposite domain when the electric field decreases to zero, as shown in figure 5(b2). Until the

opposite electric field is applied, the opposite domain appears, as shown in figure 5(b3). Due to the depinning of the domain above the dislocation array, both the remnant polarization and the coercive field at $200\,°C$ are larger than those at room temperature, as shown in figure 4(A). The evolution of domain structures in figures 5(a1)–(a4) and (b1)–(b4) shows that the unusual temperature dependence of the hysteresis loops in ferroelectric single crystal is attributed to the pinning and depinning of polarization domains by the dislocation array. When temperature increases to $600\,°C$, both the remnant polarization and the coercive field decrease due to the intrinsic low magnitude of the polarization. It is interesting to note that the remnant polarization at $E^{ex,*} = 0$ is still not zero although the temperature is above the Curie point, as shown by the curve at $T = 600\,°C$ in figure 4(A) and the domain structures in figure 5(c2). The nonzero remnant polarization above the Curie point suggests that the dislocation array would increase the apparent Curie temperature of a ferroelectric material, which has been reported recently [32, 33]. When the opposite electric field of $E^{ex,*} = -0.055$ is applied, a multi-domain appears above the dislocation arrays, as shown in figure 5(c3). The appearance of the multi-domain structure with up and down domains above the dislocation wall and the ferroelectric-to-nonferroelectric phase transition in figure 5(c3) is responsible for the double hysteresis loop at $T = 600\,°C$ in figure 4(A). The detailed mechanism is that when the temperature is higher than the Curie temperature, the region far away from the dislocation wall is nonferroelectric. Once the external electric field is applied, the field-induced phase transition from nonferroelectric to ferroelectric occurs, which results in large polarization under high electric field. When the electric field approaches zero, polarizations far from the dislocation wall become zero again. Furthermore, the average polarization of the multi-domain near the dislocation wall is also zero due to the up and down arrangement of the domains. As a result, the total polarization becomes very large when the electric field is large and very small when the electric field is close to zero, thereby leading to the double hysteresis loop. The small total polarization under low electric field leads to the double hysteresis loop. Other mechanisms have also been reported [5, 31, 34] for the double hysteresis loop. When the opposite electric field increases to the negative maximum point, the region above the dislocation array becomes a single domain again, as shown in figure 5(c4). The supplementary material (available at stacks.iop.org/SMS/23/025004/mmedia) contains movies of the temporal evolution of the polarization switching processes for cases at different temperatures with $E_0^* = 0.7$ and $E_0^* = 0.8$, respectively, in which the new domain nucleation and propagation processes are clearly shown.

The temperature dependences of the remnant polarization and coercive field with applied electric field amplitudes of $E_0^* = 0.7$ and $E_0^* = 0.8$ are determined from the simulations and plotted in figures 6(A) and (B), respectively. For the curves in figure 6(A), there is a critical temperature around $200\,°C$, below or above which both the remnant polarization and the coercive field increase or decrease with increase of temperature. If the applied electric field amplitude is 0.8,
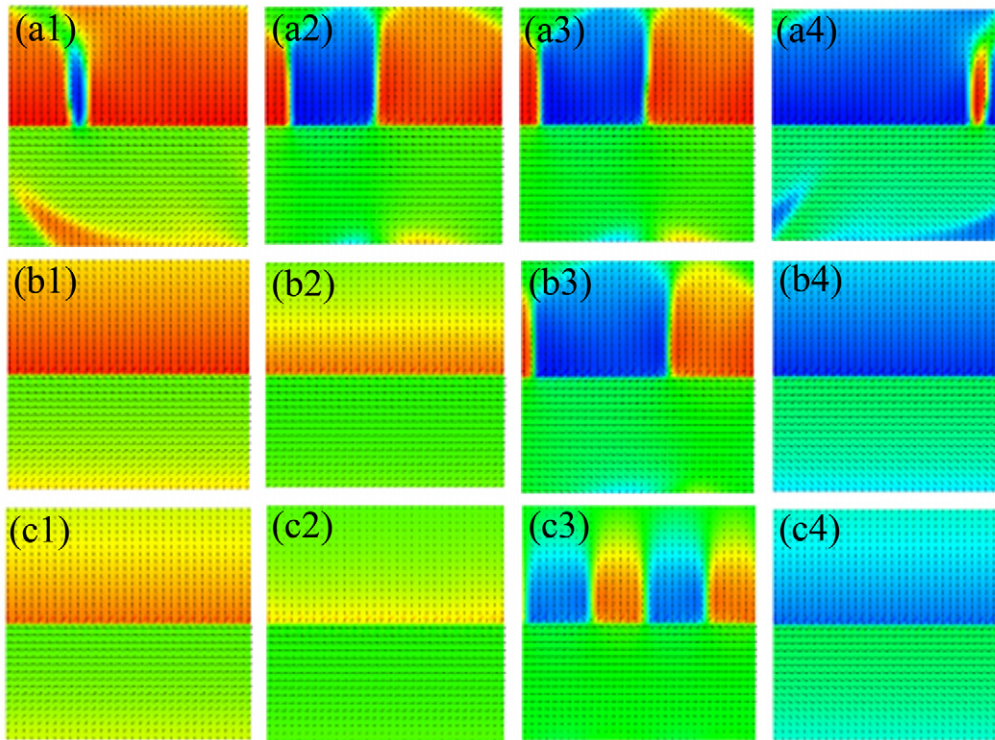
Figure 5. The domain structures (a1), (a2), (a3) and (a4) correspond to the points on the curve of $T = 25\,°C$ in figure 4(A) with $E_0^* = 0.7$, respectively; (b1), (b2), (b3) and (b4) correspond to the points on the curve of $T = 200\,°C$ in figure 4(A) with $E_0^* = 0.7$, respectively; (c1), (c2), (c3) and (c4) correspond to the points on the curve of $T = 600\,°C$ in figure 4(A) with $E_0^* = 0.7$, respectively.

however, the remnant polarization always decreases with temperature increase in the temperature range of 20–600 °C, while the coercive field increases and then decreases with temperature increase, similarly to the behavior at $E_0^* = 0.7$ in figure 6(A). The temperature dependence of the remnant polarization and coercive field with different applied electric field amplitudes implies that this is a multi-physics coupling behavior of polarizations with dislocations, applied electric field and temperature.

4. Conclusions

The temperature dependence of the remnant polarization and coercive field for a ferroelectric single crystal with dislocation arrays has been investigated through phase field simulations. In the presence of dislocation arrays, the dependence of the coercive field on the temperature is different from that of a dislocation-free ferroelectric. The coercive field increases when the temperature increases from room temperature to a critical temperature, which is inconsistent with the theoretical prediction without dislocations. This unusual phenomenon is attributed to the pinning of domain switching by the dislocation arrays. Above the critical temperature, both the coercive field and the remnant polarization decrease with increase of the temperature. Double hysteresis loops appear in the simulations when the temperature is higher than the Curie temperature, suggesting that the dislocations could change the critical temperature for the disappearance of ferroelectricity.
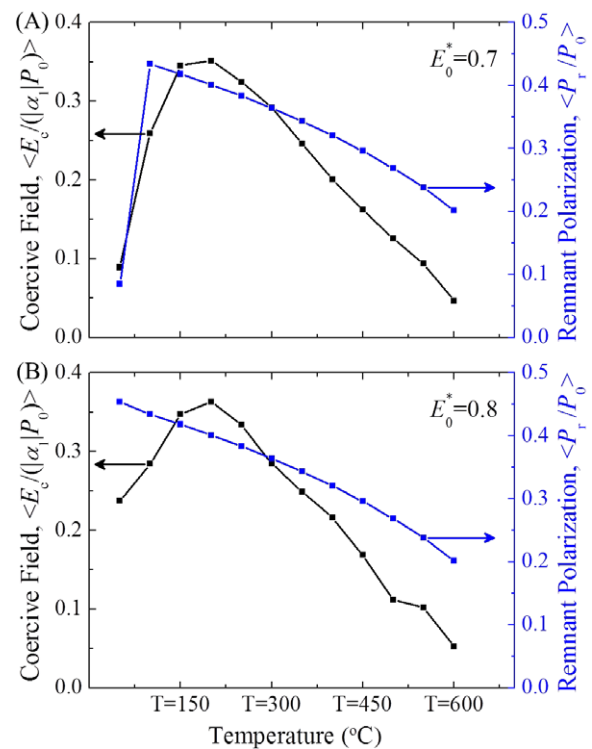

Figure 6. The dependence of the normalized coercive field ($E_c/(|\alpha_1|P_0)$) and the normalized remnant polarization (P_r/P_0) on the temperature for applied electric field amplitudes of (A) $E_0^* = 0.7$ and (B) $E_0^* = 0.8$.

References

[1] Scott J F 2007 Applications of modern ferroelectrics *Science* **315** 954–9

[2] Bondurant D W and Gnadinger F P 1989 Ferroelectrics for nonvolatile RAMs *IEEE Spectr.* **26** 30–3

[3] Khemakhema L, Maalej A, Kabadou A, Ben Salah A, Simon A and Maglione M 2008 Dielectric ferroelectric and piezoelectric properties of $BaTi_{0.975}(Zn_{1/3}Nb_{2/3})_{0.025}O_3$ ceramic *J. Alloys Compounds* **452** 441–5

[4] Lee F Y, Jo H R, Lynch C S and Pilon L 2013 Pyroelectric energy conversion using PLZT ceramics and the ferroelectric–ergodic relaxor phase transition *Smart Mater. Struct.* **22** 025038

[5] Jo W, Granzow T, Aulbach E, Rödel J and Damjanovic D 2009 Origin of the large strain response in $(K_{0.5}Na_{0.5})NbO_3$-modified $(Bi_{0.5}Na_{0.5})TiO_3–BaTiO_3$ lead-free piezoceramics *J. Appl. Phys.* **105** 094102

[6] Xu Q, Huang D P, Chen M, Chen W, Liu H X and Kim B H 2009 Effect of bismuth excess on ferroelectric and piezoelectric properties of a $(Na_{0.5}Bi_{0.5})TiO_3–BaTiO_3$ composition near the morphotropic phase boundary *J. Alloys Compounds* **471** 310–6

[7] Wu X, Liu L, Li X, Zhao X, Lin D, Luo H and Huang Y 2012 The influence of defects on ferroelectric and pyroelectric properties of $Pb(Mg_{1/3}Nb_{2/3})O_3–0.28PbTiO_3$ single crystals *Mater. Chem. Phys.* **132** 87–90

[8] Wongsaenmai S, Ananta S, Tan X and Yimnirun R 2008 Dielectric and ferroelectric properties of lead indium niobate ceramic prepared by wolframite method *Ceram. Int.* **34** 723–6

[9] Kim J S, Yoo S Y and Kim N K 2003 Dielectric characteristics of Mg-replaced $Pb[(Zn_{1/3}Ta_{2/3})_{0.2}(Zn_{1/3}Nb_{2/3})_{0.6}Ti_{0.2}]O_3$ ceramics *Mater. Res. Bull.* **38** 1957–64

[10] Li Y, Chen W, Zhou J, Xu Q, Sun H and Liao M 2005 Dielectric and ferroelectric properties of lead-free $Na_{0.5}Bi_{0.5}TiO_3–K_{0.5}Bi_{0.5}TiO_3$ ferroelectric ceramics *Ceram. Int.* **31** 139–42

[11] Kotani K, Kawayama I, Tonouchi M, Hotta Y and Tabata H 2006 Dielectric and ferroelectric properties of c-axis oriented strontium bismuth tantalate thin films applied transverse electric fields *J. Appl. Phys.* **99** 124106

[12] Bhatia B, Karthik J, Cahill D G, Martin L W and King W P 2011 High-temperature piezoresponse force microscopy *Appl. Phys. Lett.* **99** 173103

[13] Zhang S T, Yuan G L, Wang J, Chen Y F, Cheng G X and Liu Z G 2004 Temperature-dependent effect of oxygen vacancy on polarization switching of ferroelectric $Bi_{3.25}La_{0.75}Ti_3O_{12}$ thin films *Solid State Commun.* **132** 315–8

[14] Yuan G L, Liu J M, Zhang S T, Wu D, Wang Y P, Liu Z G, Chan H L W and Choy C L 2004 Low-temperature switching fatigue behavior of ferroelectric $SrBi_2Ta_2O_9$ thin films *Appl. Phys. Lett.* **84** 954

[15] Li B S, Li G R, Zhao S C, Zhu Z G and Ding A L 2005 Reorientation of defect dipoles in ferroelectric ceramics *Chin. Phys. Lett.* **22** 1236

[16] Bochenek D, Skulski R, Wawrzała P and Brzezin'ska D 2011 Dielectric and ferroelectric properties and electric conductivity of sol–gel derived PBZT ceramic *J. Alloys Compounds* **509** 5356–63

[17] Hu S Y, Li Y L and Chen L Q 2003 Effect of interfacial dislocations on ferroelectric phase stability and domain morphology in a thin film—a phase-field model *J. Appl. Phys.* **94** 2542–7

[18] Kontsos A and Landis C M 2009 Computational modeling of domain wall interaction with dislocation in ferroelectric crystals *Int. J. Solids Struct.* **46** 1491–8

[19] Zheng Y and Wang B 2006 Simulation of interface dislocations effect on polarization distribution of ferroelectric thin films *Appl. Phys. Lett.* **88** 092903

[20] Li Y L, Hu S Y, Liu Z K and Chen L Q 2002 Effect of substrate constraint on the stability and evolution of ferroelectric domain structures in thin films *Acta Mater.* **50** 395–411

[21] Wang J, Shi S Q, Chen L Q, Li Y and Zhang T Y 2004 Phase field simulations of ferroelectric/ferroelastic polarization switching *Acta Mater.* **52** 749

[22] Li Y, Li S and Zhang T Y 2009 Effect of dislocations on spinodal decomposition in Fe–Cr alloys *J. Nucl. Mater.* **395** 120–30

[23] Wu H H, Wang J, Cao S G and Zhang T Y 2013 Effect of dislocation walls on the polarization switching of a ferroelectric single crystal *Appl. Phys. Lett.* **102** 232904

[24] Wu H H, Wang J, Cao S G, Chen L Q and Zhang T Y 2013 Micro-/macro-responses of a ferroelectric single crystal with domain pinning and depinning by dislocations *J. Appl. Phys.* **114** 164108

[25] Wang J and Kamlah M 2009 Three-dimensional finite element modeling of polarization switching in a ferroelectric single domain with an impermeable notch *Smart Mater. Struct.* **18** 104008

[26] Tagantsev A K 2008 Landau expansion for ferroelectrics: which variable to use? *Ferroelectrics* **375** 19–27

[27] Woo C H and Zheng Y 2008 Depolarization in modeling nano-scale ferroelectrics using the Landau free energy functional *Appl. Phys. A* **91** 59–63

[28] Wu P, Ma X, Li Y, Gopalan V and Chen L Q 2012 Dipole spring ferroelectrics in superlattice $SrTiO_3/BaTiO_3$ thin films exhibiting constricted hysteresis loops *Appl. Phys. Lett.* **100** 092905

[29] Wang J and Zhang T Y 2006 Size effects in epitaxial ferroelectric islands and thin films *Phys. Rev.* B **73** 144107

[30] Chen L Q and Shen J 1998 Applications of semi-implicit Fourier-spectral method to phase field equations *Comput. Phys. Commun.* **108** 147–58

[31] Hussain A, Ahn C W, Ullah A, Lee J S and Kim I W 2012 Dielectric, ferroelectric and field-induced strain behavior of $K_{0.5}Na_{0.5}NbO_3$-modified $Bi_{0.5}(Na_{0.78}K_{0.22})_{0.5}TiO_3$ lead-free ceramics *Ceram. Int.* **38** 4143–9

[32] Alpay S P, Misirlioglu I B, Nagarajan V and Ramesh R 2004 Can interface dislocations degrade ferroelectric properties? *Appl. Phys. Lett.* **85** 2044

[33] Zheng Y, Wang B and Woo C H 2007 Effects of interface dislocations on properties of ferroelectric thin films *J. Mech. Phys. Solids* **55** 1661–76

[34] Merz W J 1953 Double hysteresis loop of $BaTiO_3$ at the curie point *Phys. Rev.* **91** 513–7